

THE MATHEMATICAL MODEL OF A RESISTIVE ELECTRIC SMELTING FURNACE

By J.H. Downing* and F.W. Leavitt*
(presented by Dr. Downing)

SYNOPSIS

A mathematical model of an electric smelting furnace has been developed which incorporates electrical, thermal and mass flows into a transient numerical solution. The model has been used to simulate a ferrochromium smelting operation under a variety of design and operating conditions and is in agreement with existing empirical relations for design and operation of furnaces.

This paper is a continuation of earlier studies (1,2) which provide the background for the development of the furnace model. The application of the model has been extended to include the effects of electrode spacing, electrode radius, electrode tip position and voltage on a ferrochromium smelting operation.

There are four regions, metal, slag, charge and electrode in the furnace model, whose thermal and electrical conductivities must be specified as functions of temperature.

Table 1 summarizes the thermal conductivities for the four regions. The value of metal thermal conductivity is for a 26% chrome steel in the solid state. For the slag, a constant value is assumed up to a temperature of 1873° Kelvin, which is the threshold temperature for the chemical reaction. Above 1873° the thermal conductivity is arbitrarily increased one unit for each degree of temperature above 1873°. The justification for such an increase is the enhanced conductivity due to increased mobility in the slag at elevated temperatures. Under conditions of a large temperature gradient and electromagnetic stirring, the apparent thermal conductivity of a slag was calculated to be increased up to thirty times the atomic conductivity of the slag (3). The thermal conductivity of the charge is calculated by assuming that only radiative transfer is occurring into a porous bed. Within the bed, the thermal conductivity of the solids was 8.65 joules/ms⁰K, the particle size .038 meters, and the emissivity unity. The void fraction was 0.3.

The thermal conductivity of the electrode was considered to be constant up to a temperature of 2273°K and characteristic of carbon electrodes. Over 2273°K the thermal conductivity was increased to that of graphite on the assumption that graphitization would proceed over this temperature.

* Metals Division, Union Carbide Corporation, USA

TABLE 1 - THERMAL CONDUCTIVITIES

Substance	Formula	joules/meter sec °K		Reference
		Temp. Range °K		
Metal	$0.0168 \times T$			Handbook of Physico-Chem. Prop. of Molten Iron & Slag. Inst. of Iron & Steel of Japan # 12 (1973)
Slag	1.73 $1.73 + (T-1873)$	< 1873 > 1873		Szekely, J. AICHE - IChem. E. Sym. Ser. #2 (1965)
Charge	$1.73 [Z + 0.7 / (0.2 + 1/Z)]$ $Z = 2.595 \times 10^{-10} \times (T^{\circ R})^3$ (T ^{°R} temperature degrees Rankine)			Schotte, W. AICHE J. 6 # 1 (1960) 63
Electrode	15.57 122.83	< 2273 > 2273		Carbon Products Pocket Handbook U.C.C. (1964)

Electrical resistivities are given in Table II. The metallic electrical resistivity is that of chromium. The slag, whose resistivity is given in Table II, contains 40% silica, 30% magnesia, and 30% alumina. The formula is derived from the 1700°C and 1800°C measurements assuming a linear relationship between the logarithm of the resistivity and the reciprocal of the absolute temperature.

The electrical resistivity of the charge was taken from data measured at our laboratories. This formula was derived from data obtained on a coke of 8 x 20 mesh size. The measurements, which were described in an earlier paper (4), were extended up to 1700°C. The size of the coke is smaller than is typical for furnace feed. Although larger coke would be less resistive, the presence of non-conducting ore increases resistivity. More reliable values for this crucial property would be desirable. The resistivity of the electrode has two values; one for carbon at temperatures under 2273°K, the other for graphite above 2273°K.

The rate of the chemical reaction $k = 125.94 \exp(-27000/T)$ 1/sec. is the same as in earlier work (1,2). The activation energy was derived by taking an average value from the study of fourteen different chrome ores (5). The preexponential term was evaluated by assuming that the reaction is complete in one hour at 1873°K.

Minor changes have been made in the model. The results of the simulation of a furnace with an electrode of .445 meters radius on a pitch radius of 1.18 meters, operating at a voltage of 120, showed that there was little interaction between adjacent electrodes. If this is true only three planes are required instead of seven as is illustrated in Figure 1. There are two bounding planes along the diameter of the electrode, and one active plane at 90° to these planes.

TABLE II - ELECTRICAL RESISTIVITIES (ohm meters)

<u>Substance</u>	<u>Formula</u>	<u>Temp. Range °K</u>	<u>Reference</u>
Metal	$5 \times 10^{-8} + 0.567 \times 10^{-8} (T-273)$		Baum, B.A. et al. Izv. Akad. Nauk SSSR, Met. Gorn. Dolo. 1964 (2) 149-55 (CA <u>61</u> 2572)
Slag	$1.3295 \times 10^{-5} \exp (1.375 \times 10^4 / T)$		Liutikov, R.A., Tsylev, L.R. Russian Mining & Metall. #1 (1963) 12
Charge	$2.565 \times 10^5 / T^{2.0554}$		
Electrode	5.08×10^{-5} 1.04×10^{-5}	< 2273 > 2273	Carbon Products Pocket Handbook U.C.C. (1964)

Reducing the number of planes reduces the computing time. Previously 3,000 seconds of real time had been simulated.

The criteria for a steady-state were the reduction in the increase of the maximum temperature and in the energy input. The longer the duration of the simulation the closer the results will be to steady-state. Therefore, either taking larger time steps for each iteration or performing fewer calculations during each iteration leads to a longer simulated real time and a more accurate result.

It had been necessary to introduce a very high resistance region under the electrodes. This high resistance region extended out to the last radial position in the electrode. The final radial position under the electrode was assigned the resistivity value of the region in which it is located. However, reactive material was not permitted to enter this radial position. The result was that high temperatures existed in this region and in the electrode itself.

On the small furnace, this model functioned reasonably well. However, in larger units, leaving the final radial position underneath the electrode at relatively low resistivity led to extremely high temperatures both in that region and in the electrode. Therefore, all radial positions under the electrode were assigned a high resistivity. This forces the current to flow to the outside of the electrode and feed-off into the regions at the side of the electrode.

The physical justification of high resistance under the electrode is an attempt to simulate the skin effect in the electrode. Also the restriction of charge flow to the vertical direction necessitates negligible power

generation in the sub-electrode region because there is no mechanism for energy absorption there. The concept of vertical plug flow has recently received support (6).

The model can be substantiated by simulating existing furnaces and comparing the results of the simulations with actual operations. This was done for a relatively small unit (1,2). Data is available for a larger furnace whose characteristics are given in Table III. The internal structure of the furnace, shown in Figure 2a, has a slag-metal interface at 0.3m and the slag-charge interface at 0.74m.

TABLE III - CHARACTERISTICS OF FURNACE PRODUCING FERROCHROMIUM

Radius of Electrode (m)	0.635
Radius of Furnace (m)	4.88
Pitch Radius (m)	1.70
Depth (m)	2.70
In-phase Voltage	150
Power Kw	25,000
k Ω in.	0.42

The furnace is fed a mixture of ore, flux, and reducing agent. In this simulation, a low chrome-iron ratio ore was used. The metal produced contained 54.5% chromium, 34.5% iron, 5% silicon, and 6% carbon. The slag, resulting from the reduction, contained 34% silica, 4.1% calcium oxide, 33.0% aluminium oxide, and 28.8% magnesium oxide.

The position of the electrode tip relative to the slag and metal surfaces is an important variable. In the previous work it was determined that the tip could not be immersed in the slag because the furnace would be too conductive. On the other hand suspending the electrode high in the furnace makes the furnace too resistive.

Simulations have been made with tip positions of 0.74m, 0.78m and 0.9m. The vertical points (see Fig. 2a) are Z(1)=0, Z(2)=0.13, Z(3)=0.26, Z(4)=0.34, Z(5)=0.44, Z(6)=0.54, Z(7)=0.64, Z(8)=0.72, Z(9)=0.76, Z(10)=0.80, Z(11)=1.0, Z(12)=1.4, Z(13)=2.0, Z(14)=2.7, Z(15)=3.212, Z(16)=3.724. The metal-slag interface is between Z(3) and Z(4); the slag-charge interface between Z(8) and Z(9).

If the electrode tip position is at 0.74, the electrode is in contact with the slag because there is no intervening charge. If the tip is situated at 0.78 there will be one vertical point, Z(9), in the charge between the electrode and the slag. If the tip is placed at 0.9 there will be two points Z(9) and Z(10) in the charge between the tip and the slag. The results of the simulation are shown in Table IV, which follows.

The results can be compared with the furnace in Table III. Placing the electrode near the slag-charge interface results in a load and "k" close to practice. With the electrode in the low position the power drawn is too high and the "k" is low. On the other hand too high a position leads to low power and high "k".

TABLE IV - COMPARISON OF TIP POSITION

Furnace with 0.635 m radius electrodes, operating
at 150 volts, time of simulation 20000 sec.

<u>Run</u>	<u>Tip m</u>	<u>KW</u>	<u>k Ωin.</u>	<u>KW/cm²</u>	<u>Max T^oK Elect.</u>	<u>Max T^oK Charge</u>	<u>Max T^oK Slag</u>	<u>Max T^oK Metal</u>	<u>Kg metal/ 1000 sec.</u>	<u>KWH/ kg</u>
A	.74	31650	0.34	.83	2477	2378	2396	2305	424	3.45
B	.78	22710	0.47	.60	2527	2429	2325	2126	292	3.61
C	.90	16170	0.66	.43	2312	2219	2103	1937	198	3.78

The highest electrode and charge temperatures occur at the intermediate position. In the lower position the slag and metal temperatures are highest and the slag temperature exceeds the charge temperature.

Table V shows the change in simulation B with time. The irregular variation in the electrode temperature and power may be due to the step change in electrode properties. If graphite properties are used throughout the electrode, a steady decrease in the rate of electrode temperature and power is calculated.

TABLE V - CHANGE OF TEMPERATURES AND LOSSES FROM RUN B AS A FUNCTION OF TIME

<u>Time</u> <u>Secs.</u>	<u>Max.</u> <u>Elect.</u> <u>Temp.</u>	<u>Max.</u> <u>Charge</u> <u>Temp.</u>	<u>Max.</u> <u>Slag</u> <u>Temp.</u>	<u>Max.</u> <u>Metal</u> <u>Temp.</u>	<u>Bot. Loss</u> <u>KW</u>	<u>Top Loss</u> <u>KW</u>	<u>Elect.</u> <u>Loss KW</u>	<u>KW</u> <u>Sector</u>
0	1831	1859	1873	1873	0	0	0	0
4000	2502	2409	2304	2101	273.9	44.8	5.9	3505
8000	2519	2416	2314	2116	265.5	45.4	23.2	3592
12000	2520	2421	2318	2120	259.0	47.1	37.1	3662
16000	2521	2426	2321	2123	253.3	49.9	47.2	3738
20000	2527	2429	2324	2126	248	53.5	53.3	3785

The bottom loss is decreasing while the top loss and loss off the electrode surface above the mix are increasing. The bottom loss is still being influenced by the initial temperature.

The slow increase in power and temperature are associated with small changes in the furnace which will take a long time to come to equilibrium. Therefore, although convergence to a steady-state has not been demonstrated, results at 20,000 seconds of simulated time will be compared on the assumption that equilibrium is sufficiently close that valid comparisons can be made.

In Table IV the best electrical efficiency is calculated for the low tip position although this leads to a relatively lower "k" and higher power than the actual operating unit described in Table III. The calculated losses for the three runs are shown in Table IV. The improved efficiency in A is due to relatively low losses compared to metal production.

Placing the electrode tip in the slag layer resulted in increasing temperatures leading into an unstable solution.

Based on these results the ideal operating situation would be one in which the electrode just contacted the slag. The assumed constant, horizontal slag-charge interface is not found in practice because among other things the products of reaction are not continuously removed. Therefore, operation at a position somewhat above the slag-charge interface is probably an

operating necessity. The balance of the calculations will be made with the electrode positioned above the slag-charge interface.

In Figure 2b the temperatures in the electrode (the first four radial points) are highest in the center and are cooled by the mix except at the tip where the highest temperature in the furnace occurs on the outside of the electrode. The temperature in the charge goes through a minimum at constant, Z. The charge nearest the electrode is heated by the electrode; the temperature in the next radial element is lowered by the flow of mix to the reaction zone. The metallic zone (the first 3 Z positions) is cooler than the slag due to losses out of the furnace bottom and negligible energy generation.

The voltage in Figure 2c decreases slightly down the length of the electrode. The metal is at essentially zero voltage.

The energy generation in Figure 2d is concentrated near the electrode tip in the slag, charge and electrode.

The distribution of the energy in the four regions of the furnace is 1.84% metal, 28.5% slag, 54.7% charge, 15.0% electrode. Although the energy generated in the electrode is small it must be conducted into the adjacent regions because there is no mechanism for absorption at steady-state within the electrode.

The response of the model to voltage change is shown in Table VII which follows. Increasing voltage leads to increasing power in the sector, which is 1/6 of the furnace. The K-factor drops from .5 at 130 volts to .43 at 170 volts. The maximum temperatures in the various regions in the furnace are also given. At higher voltages the temperatures in the various regions are higher.

The enthalpy of the products, which includes the heat of reduction and the sensible heat and fusion energy of the products, is calculated as an average rate for the period. From the weight of the metal and nonreducible oxides produced, and the enthalpy for these species, it is possible with an energy balance to calculate an average temperature for the products. This temperature increases with power density.

Ninety percent of the electrical energy introduced is accounted for in the enthalpy of the products and the losses. The energy in the carbon monoxide gas has been estimated by taking the average top surface temperature as the mean temperature of the carbon monoxide leaving the furnace and amounts to approximately 6% of the input power, which accounts for much of the difference between the computed losses and the input energy.

The greatest amount of energy is consumed per unit of alloy produced at the low voltage. This is due to the thermal losses from the bottom of the furnace which are essentially the same in this run as in the higher powered runs and yet much less metal is produced at the low voltage. The relatively more efficient operation, simulation B', with the graphite electrode at 150 volts is due to the low loss from the electrode. The loss from the top of the furnace is slowly increasing, reflecting increased temperatures in this region of the furnace.

Calculated "k" is plotted against power density in Figure 3. Also displayed over a limited range of power densities are the empirical results on ferrochromium obtained by Kelly (7) which "do not represent all of the random

TABLE VI - LOSSES AT 20,000 secs.

<u>Run</u>	<u>Tip</u>	<u>Bot. Loss KW</u>	<u>Top Loss KW</u>	<u>Elect. Loss KW</u>
A	.74	253	71	143.0
B	.78	248	53.5	53.3
C	.80	244	58	12.0

TABLE VII - ELECTRODE RAD.=.635m, TIP POSITION = 0.78m, TIME = 20,000 Secs.

<u>Run</u>	<u>Volt.</u>	<u>KW/ Sect.</u>	<u>kΩin.</u>	<u>KW/cm²</u>	<u>Amp/cm²</u>	<u>Max T^oK Elect.</u>	<u>Max T^oK charge</u>	<u>Kg Met/ 1000 Sec.</u>	<u>KWH/kg</u>	<u>Enthal of liq. KW</u>	<u>Bot. Loss KW</u>	<u>Top Loss KW</u>	<u>Elect. Loss KW</u>	<u>Avg. Prod. Temp.</u>	<u>% Energy Acct. for</u>
D	130	2630	0.50	0.42	3.19	2404	2332	194	3.76	1992	246	50	28	2028	88.1
B	150	3785	0.47	0.60	3.98	2527	2429	292	3.60	3028	248	53.5	53.5	2070	89.4
B'	150	3847	0.46	0.61	4.05	2528	2447	312	3.43	3245	248	54	5	2085	92
E	170	5250	0.43	0.83	4.88	2717	2525	422	3.46	4422	252	58	93	2127	92

1
0
1

operating experience available. Rather, they are selected data representing what is known to be satisfactory working areas for fully competitive performance."

On this basis a calculated "k" for any given condition might not correspond to the ideal conditions given by the empirical relations of Kelly.

The set A,B,C shows the variation of "k" with tip position. C definitely appears to be outside of the preferred "k" range. B and B' are slightly above the preferred "k". The line joining A and B is roughly parallel to the optimum "k" line, however it was agreed above, that tip positions closer to the slag than B might be difficult to maintain and therefore tip position B is optimal.

Varying voltage with the tip at 0.78 meters leads to the set D,B,E. D is an under utilization of the electrode, which leads to a relatively high specific energy consumption because of high losses and low metal production. In Run E excessively high temperatures are developing in the electrode and in the charge and slag in the vicinity of the electrode tip. These could lead to undesirable side reactions which could penalize efficiency. The loss into the electrode is already becoming a factor. Run B', in which graphite electrodes were used has a better efficiency because losses from the electrode are reduced and the reaction products are at lower temperature than E.

The limitation on voltage appears to arise from the inability of the electrode to carry the additional current without overheating.

Because the model predicts the behavior of an operating furnace reasonably well it can be applied to the simulation of furnaces differing from those now in use.

Simulations were carried out of a furnace larger than any currently employed. This was done by doubling all of the radial dimensions of the previously modelled furnace. The vertical dimensions including the position of the tip of the electrode remained the same. The radius of the electrode, the pitch circle radius and the pitch circle furnace radius were 1.27, 3.4 and 9.76 meters. The voltage applied to the electrode ranged from 150 - 230 volts. The results are seen in Table VIII which follows. At 150 volts, the electrode is seen to be underpowered with a power density of only 0.23 kilowatts per cm^2 .

This low power density leads to a high k-value of .61. The maximum temperatures within the furnace are reduced. As the voltage is increased to 230 volts, the k drops to .48 and the temperatures in the furnace increase. The values for k as a function of power density are displayed in Figure 3.

Points F, G and H are in agreement with the empirical values. Point I however deviates. This is the result of the reaction rate increasing more rapidly with temperature than the resistivity in the charge zone. The major effect of increasing power is in the high temperature in the electrode at relatively low power density.

In Table VIII, Run J, in the smaller electrode the maximum temperature is only 2549^oK compared to 2849 or 3157^oK for the larger electrode at comparable power density.

The mechanism by which the electrode can lose energy to the charge is by radiation. As the diameter of the electrode increases the volume in which electrical energy is converted to heat energy increases more rapidly than the surface through which such energy must be dissipated, leading to higher temperatures in the larger electrodes for the same power density. These higher temperatures are transmitted to the charge leading to its super-heating.

All of the estimations using three-plane geometry assume that the power feeds off the electrode symmetrically. Employment of three planes was prompted by the desire to extend the simulated time as much as possible in an attempt to reach a steady-state. If there is asymmetry in power distribution within the furnace, more planes are required. The simulation in the original work (1,2) was repeated excluding the last radial position under the electrode from electrical conduction by specifying high resistivity at that location.

Using three planes, Run J, instead of seven planes, Run K, leads to a simulation in which there is slightly greater power and a lower k-factor. Some of this discrepancy may be due to differences in boundary geometry between the two simulations. It also may be the result of asymmetry. A detailed examination of the 7 plane simulation, Run K, shows asymmetry exists.

Comparing temperatures in Run K at the outside of the electrode, along plane two with those along plane six shows the temperatures in plane two are higher than those in plane six. This suggests that with a pitch circle radius of 1.18 there is a tendency for some preferential flow of current from the electrode toward the center of the furnace or the other electrode.

In order to investigate this effect more closely the pitch circle diameter was lowered to one in Run L. The other conditions were kept the same. The results are seen in Table IX which follows.

The power has increased and "k" has dropped, the maximum temperature in the electrode is higher and is located in Plane 2. Similarly, the maximum temperature in the charge is higher, and is also located in Plane 2. In addition to the asymmetry due to the presence of another electrode, asymmetry can be induced by bringing the furnace wall close to the electrode. Current, instead of flowing straight down or across toward the other electrode, tends to short to the wall which is at zero voltage relative to the electrode.

In simulation M, the pitch radius is 1.18 meters, but the radius of the furnace has been reduced from three meters to two. The response of k and power is similar to the case of reduced pitch radius. The maximum temperatures in the electrode and charge are higher than in the normal run, however, the maximum temperatures are in Plane 6, not Plane 2.

Three-dimensional representations of the temperature in Plane 2 and 6 for the three cases are shown in Figure 4a - e. The asymmetry introduced into the furnace by these changes in geometrical factors can be seen. The relative importance of the proximity of another electrode or a conductive surface like the furnace wall to the electrode would vary, with the physical properties of the mix materials and the relative position of the tip of the electrode to the metallic conductor in the bottom of the furnace. For instance if the electrode were higher in the furnace it would be anticipated that the spacing or the furnace radius would be more critical than if the tip were low in the furnace near the metallic conductor.

TABLE VIII - ELECTRODE RAD.=1.27 m, PITCH RAD.=3.4 METERS

TIME=2000 SECS.

Run	Volt.	KW/ Sect.	k Ω in.	KW/ cm ²	Amp/ cm ²	Max.T Elect.	Max.T Charge	Kg Met. 1000 sec.	KWH/ kg	Enthal. Liq. KW	Bot. Loss	Top Loss	Elect Loss	Avg.T Prod.	%Power Acct.
F	150	5759	.61	0.23	1.52	2431	2251	417	3.84	4313	974	164	46	2052	95
G	170	7981	.57	0.32	1.85	2578	2319	580	3.82	6055	979	168	93	2104	91
H	200	12367	.51	0.49	2.44	2849	2420	903	3.80	9563	985	175	234	2185	89
I	230	17491	.48	0.69	3.01	3157	2767	1330	3.65	14288	991	195	300	2264	90
Electrode rad.=.4445 m; Pitch rad.=1.18 m															
J	120	1879	.42	0.61	5.09	2549	2581	146	3.56	1420	149	45	24	1871	87.2

TABLE IX - ELECTRODE RAD.=.4445, VOLTAGE=120 VOLTS, TIME=10,000 SECS.

Run	Pitch Rad,m	Furn. Rad,m	KW/ Sect.	7 Planes		Amp/ cm ²	Max.T Elect.	Max.T Charge	Kg Met/ 1000 Sec.	KWH/kg
				k Ω in.	KW/cm ²					
K	1.18	3	1820	.435	0.59	4.88	2546	2566	141.6	3.50
L	1.0	3	1965	.40	0.63	5.29	2568	2594	152.4	3.59
M	1.18	2	1974	.40	0.64	5.30	2578	2602	154.8	3.54
3 Planes										
J	1.18	3	1879	.42	0.61	5.05	2549	2581	146	3.56

The fact that asymmetry can exist around the electrode leads to the concept of optimum spacing and optimum reaction zones for a given product and size of furnace.

The model can be used to calculate the reaction zone. The total charge fed to any vertical column in the furnace can be determined. This charge replenishes the mix consumed during the interval by reaction. The numerical solution gives discrete results at a given radial and angular position, which can be converted to a continuous function by curve fitting.

The analytical expression best describing the relationship between feed rate and the distance from the center of the electrode, r , was the exponential function, $f=Ae^{Br}$. Where f is the flow rate in units of $\text{kg ore/m}^2 \text{ sec}$. Table X, which follows, lists the constants for the various simulations.

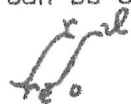
The reaction zone can be described in various ways. It could be imagined to encompass a region containing linear velocities of mix travel greater than some limit. The linear velocity is obtained by dividing the feed rate by the bulk density of the ore, 3195.5 kg/m^3 . The distance $r(v)$ at which a linear velocity of 2.54 cm/hr is attained is given in Table X.

TABLE X

Run	$f=Ae^{Br}$ ($\text{kg ore/m}^2 \text{ sec}$)		$r(v)$	$r(v)$	$r(99)$	$r(99)$
	A	B	$\sqrt{2.54} \text{ cm/hr}$	$r(\text{pitch})$	reaction 99% compl.	$r(\text{pitch})$
B	35.57	-5.290	1.39	.82	1.66	.98
B'	38.23	-5.298	1.40	.82	1.66	.98
D	56.50	-6.037	1.29	.76	1.52	.89
E	50.14	-5.280	1.46	.86	1.66	.99
C	9.33	-4.205	1.43	.84	1.95	1.15
A	106.03	-6.067	1.39	.82	1.52	.89
J	23.67	-7.425	.94	.80	1.18	1.00
K(2)	17.46	-6.32	1.05	.89	1.31	1.17
K(6)	34.41	-7.647	.96	(.53)	1.15	(.63)
L(2)	9.88	-4.759	1.28	1.08	1.63	1.38
L(6)	33.11	-7.579	.96	(.53)	1.16	(.64)
M(2)	17.99	-6.378	1.05	.89	1.31	1.11
M(6)	21.16	-6.159	1.11	(1.35)	1.34	(1.63)
F	486.255	-4.883	2.04	.60	2.32	.68
G	570.81	-4.786	2.12	.62	2.35	.69
H	748.76	-4.677	2.23	.66	2.37	.70
I	997.04	-4.613	2.32	.68	2.39	.70

() $r(v)$ or $r(99)/[r(\text{furnace})-r(\text{pitch})]$

Another way of defining the reaction zone is that distance within which a given fraction of the total reaction has been completed. The amount reacted can be obtained by integrating f throughout the area outside the electrode.



$\int_{r_e}^r f r dr d\alpha$. Where r_e is the radius of the electrode. The fraction reacted, F , at any radius r is obtained by dividing the above integral by

the integral evaluated at $r = \infty$ at which condition $F = 1$.
$$F = \frac{1 - e^{-Br}(Br-1)}{e^{-Bre}(Bre-1)}$$

This equation can be solved for r at a given F . Table X gives the distance r (99) within which 99% of the reaction occurs.

In 3 plane simulation the interaction with the other electrodes is neglected. The reaction zone in this case is symmetrical about the electrode.

In simulations K-M, directionality is observed and the reaction zone is distorted. The distortion is small in Run K, but becomes appreciable in L and M where the influence of the adjacent electrode and wall respectively become evident.

In L(2) both distances, $r(v)$ and $r(99)$, are seen to exceed the pitch radius whereas in the other simulations the radii are less than the pitch radius. Similarly in M(6) the distance from the electrode center to the wall, 0.82 meters, is exceeded by the reaction distance in Plane 6.

If the comparison of the reaction distance with the pitch radius or distance from the electrode center to the wall is indicative of proper spacing or furnace radius the largest electrode (F,G,H,I) is further from interaction than the other sizes and could be at a closer spacing.

The reaction distance increases slightly with power. Figure 5 shows $r(v)$ for two different electrodes as a function of power density.

Raising the electrode also leads to increased reaction distance. This is apparent by comparing Run C with runs A and B. Kelly (8) has given a ratio of optimum reaction zone for various products. This ratio, defined as $[r(\text{pitch})/r(\text{electrode})]^2$, has been empirically determined to be 6-8 for ferrochromium. The value for the three electrode sizes is approximately 7.1. Only the close spacing of Run L with a ratio of 5.05 falls outside the range. In an earlier paper Kelly (7) defined $r(\text{furnace}) = 2.29 \cdot r(\text{pitch})$. For the given furnace this criterion is $r(\text{furnace}) = 2.70$ m. Reducing the furnace radius to 2.0m violated this criterion. Therefore, the model is in agreement with these empirical spacing laws because appreciable interaction was calculated when values outside the recommended $r(\text{pitch})$ and $r(\text{furnace})$ were used. Whereas the reaction distance was calculated to be close to the appropriate dimensions in the preferred empirical ranges.

CONCLUSIONS

The resistive model of an electric smelting furnace has been applied to the investigation of design and operating parameters. The design parameters studied include electrode size, electrode spacing and furnace diameter. Operating parameters investigated were voltage, tip position and electrode materials. The results were compared with operating data and were in general agreement.

In modeling a large hypothetical furnace it was determined that high electrode temperatures would be a problem particularly if current densities similar to those in smaller electrodes were used.

The necessity of assuming high resistance under the electrode, intensified thermal conductivity in the slag and the poor quality of physical property data weaken the conclusions which can be drawn from the simulations. On the other hand successful simulations of existing units and agreement with empirical laws lend support to the validity of the calculation.

The model assumes the conduction occurs through resistance of complicated geometry, which vary with temperature. Ferrochromium smelting is largely in the ohmic regime (9) which may explain the success of this simulation. Extension to other systems whose mode of conduction is less well understood, i.e. silicon smelting, may prove to be difficult.

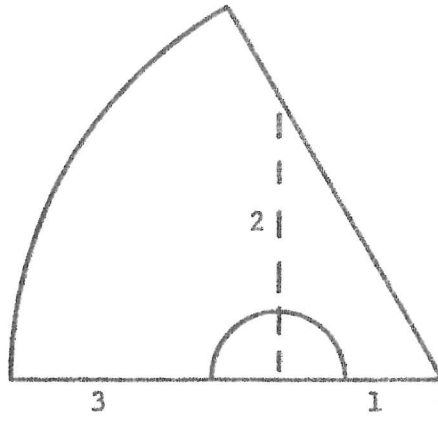
Where it does apply, the model provides theoretical background for the design, operation and control of electric smelting furnaces. This background will be useful in the further development and optimization of this smelting technique.

BIBLIOGRAPHY

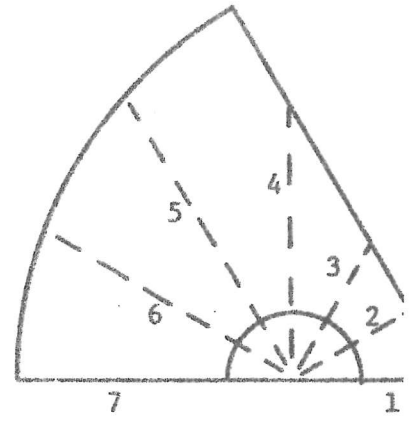
1. DOWNING, J.H.: World Electrotechnical Congress Moscow, (1977) Section 4A paper 16.
2. DOWNING, J.H.
LEAVITT, F.W.: Electric Furnace Proceedings 36 (1978) 209.
3. DILAWARI, A.H.
SZEKELY, J.: Met. Trans. B 90 (1978) 77.
4. DOWNING, J.H.
URBAN, L.: Journal of Metals (1966) 337.
5. BARCZA, N.A.: Electric Furnace Proceedings (1971)
et.al. 88.
6. SEE, J.B.: NIM Report #1967.
7. KELLY, W.M.: Carbon and Graphite News, Vol. 5
#1 (1958).
8. KELLY, W.M.: International Sym. Ferroalloys and
Silicon Metal, Sibenik, Yugoslavia
(1975).
9. RENNIE, M.S.: Electric Furnace Proceedings (1979)
to be published.

Figure 1

Three Plane



Seven Plane



Furnace Grid

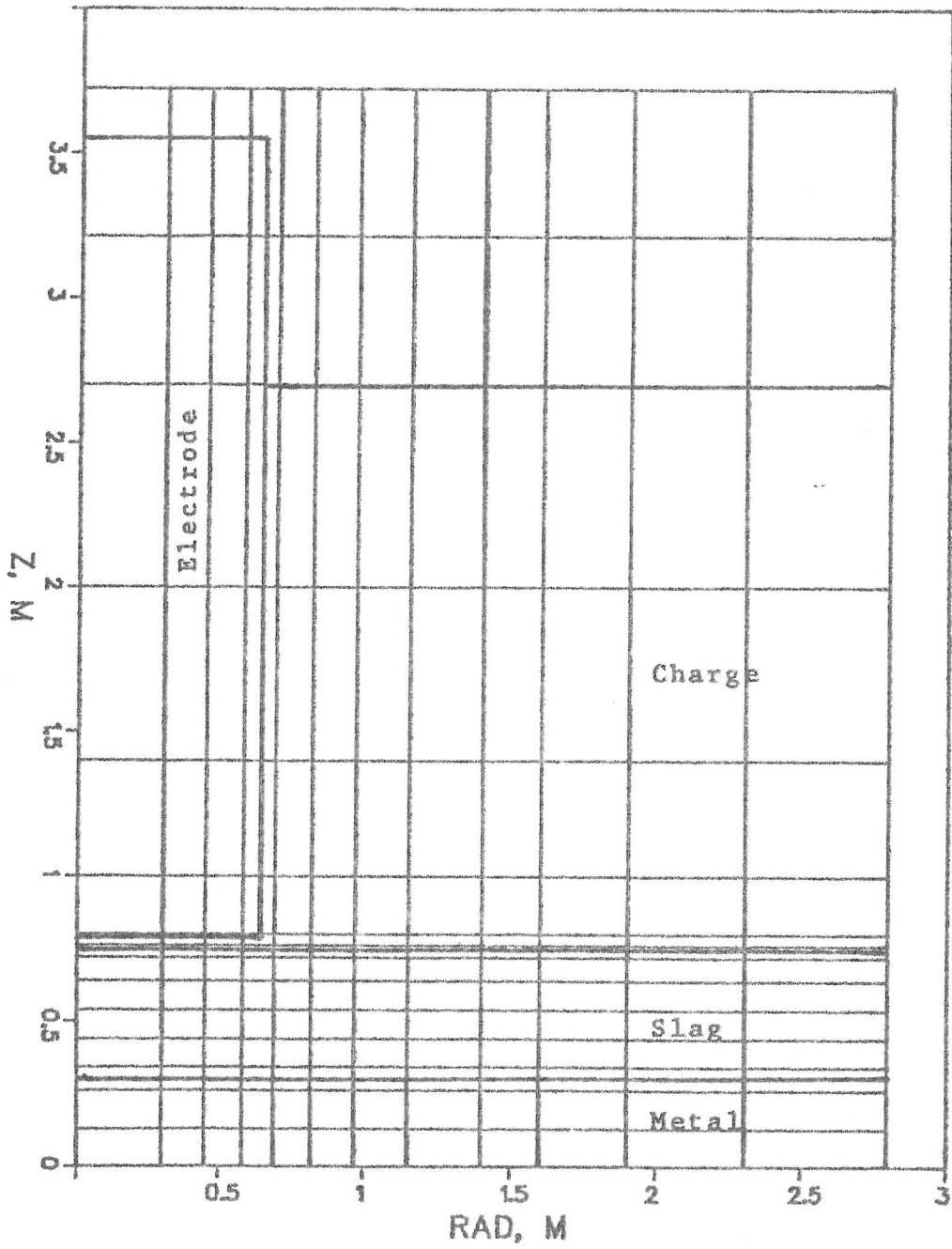


Figure 2b

Temperature

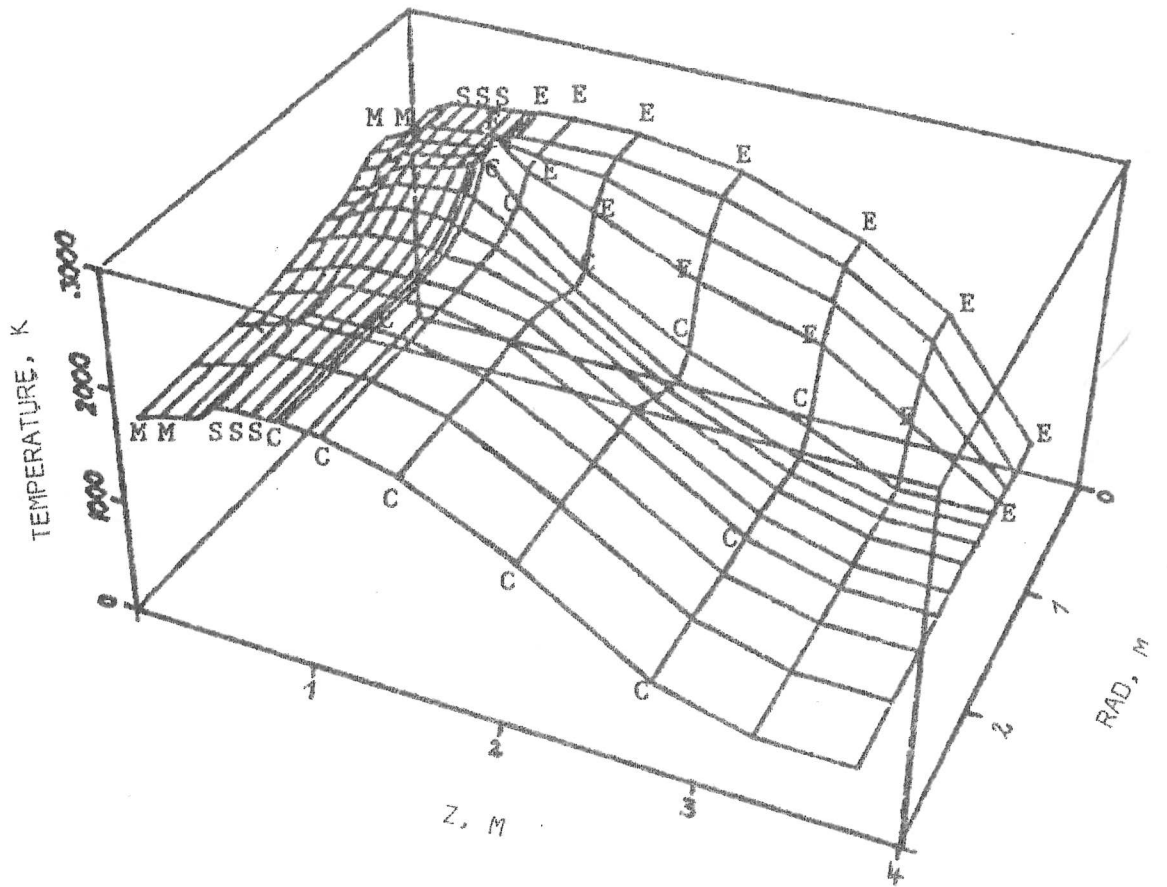


Figure 2c

Voltage

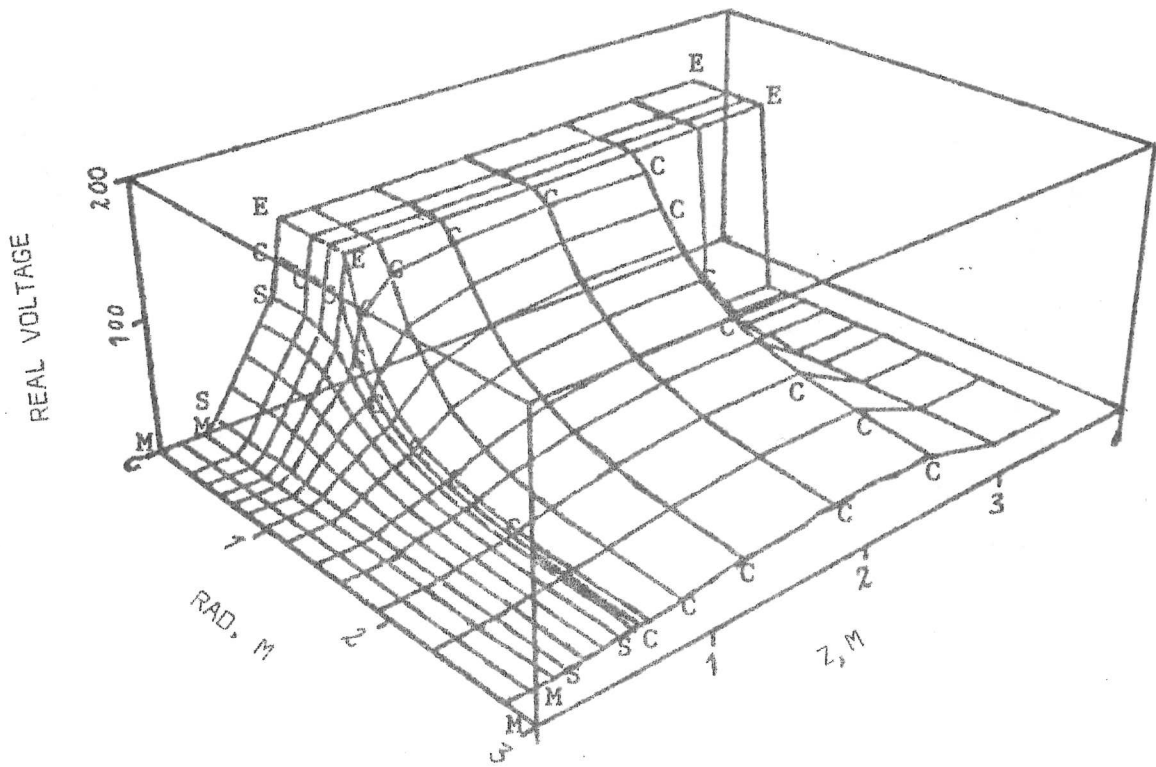


Figure 2d

Rate of Energy Generation

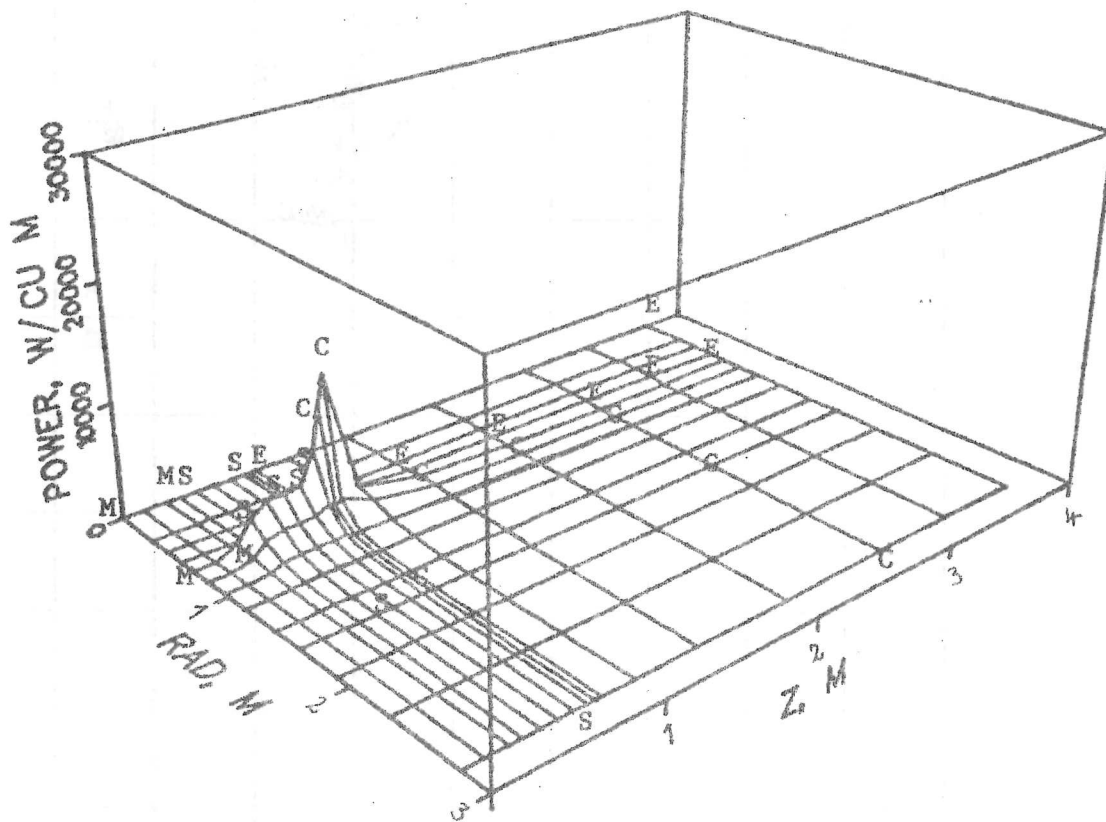


Figure 3

"k" versus Power Density

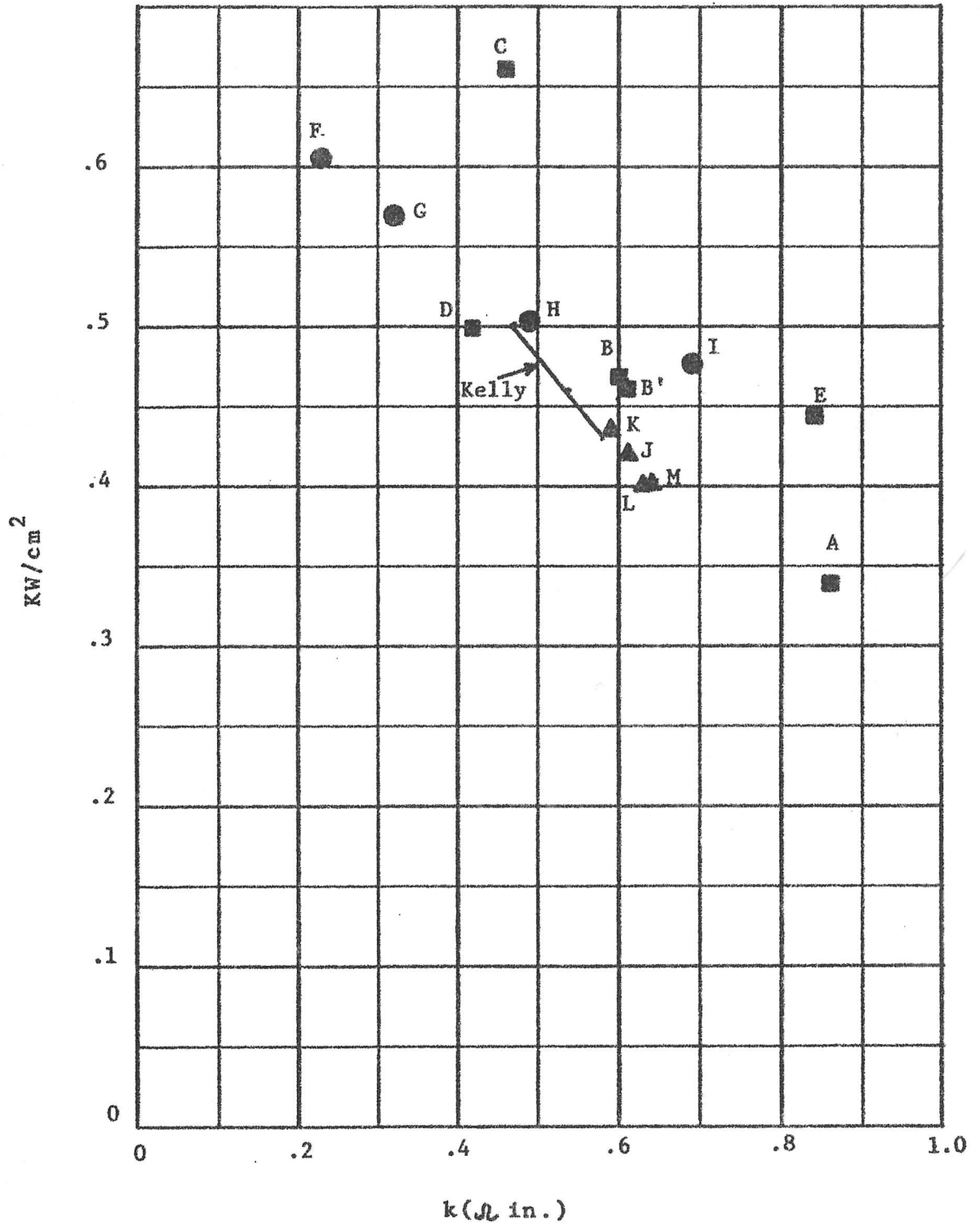


Figure 4a

Furnace Grid

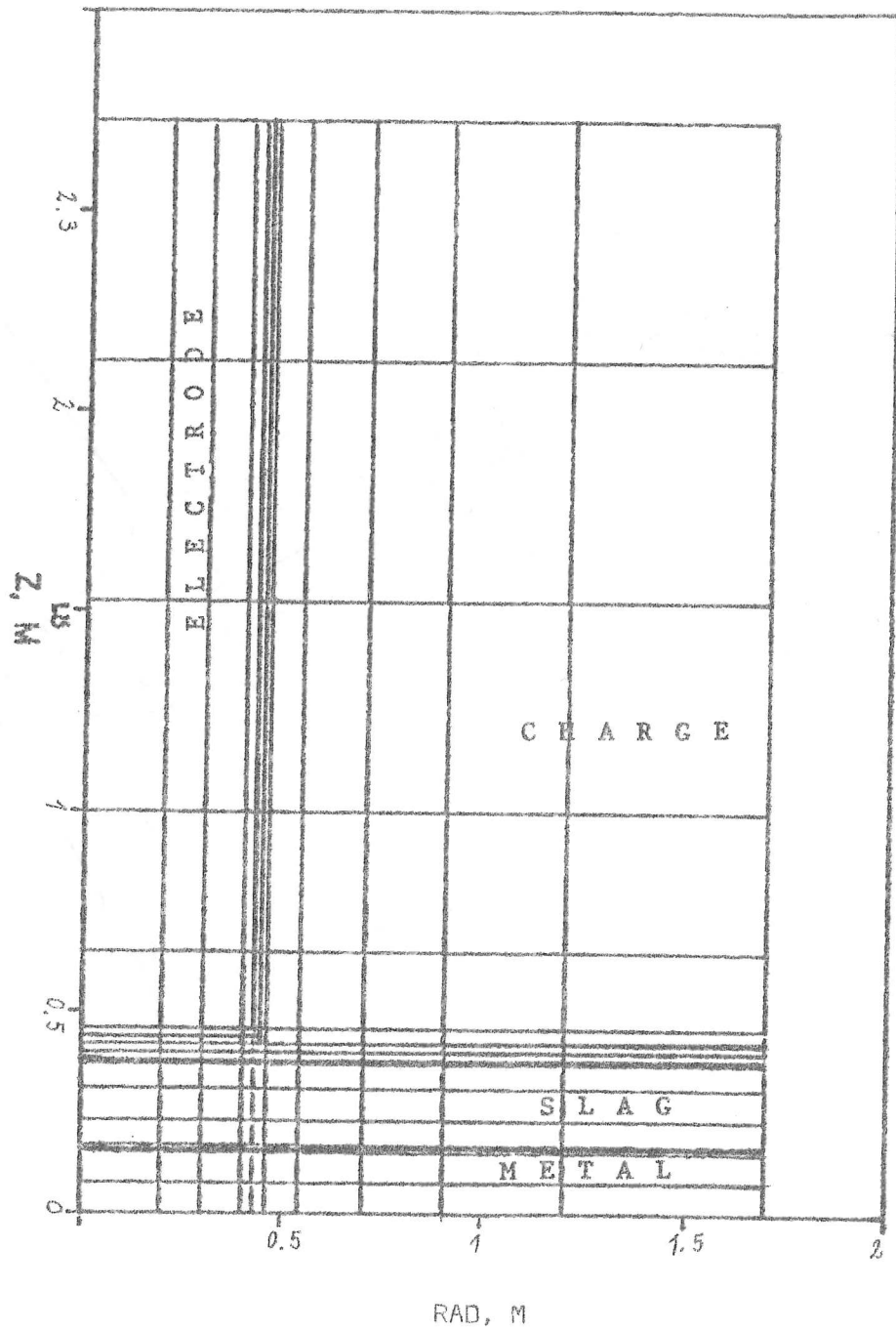


Figure 4b

BASE CASE, ANGLE 2

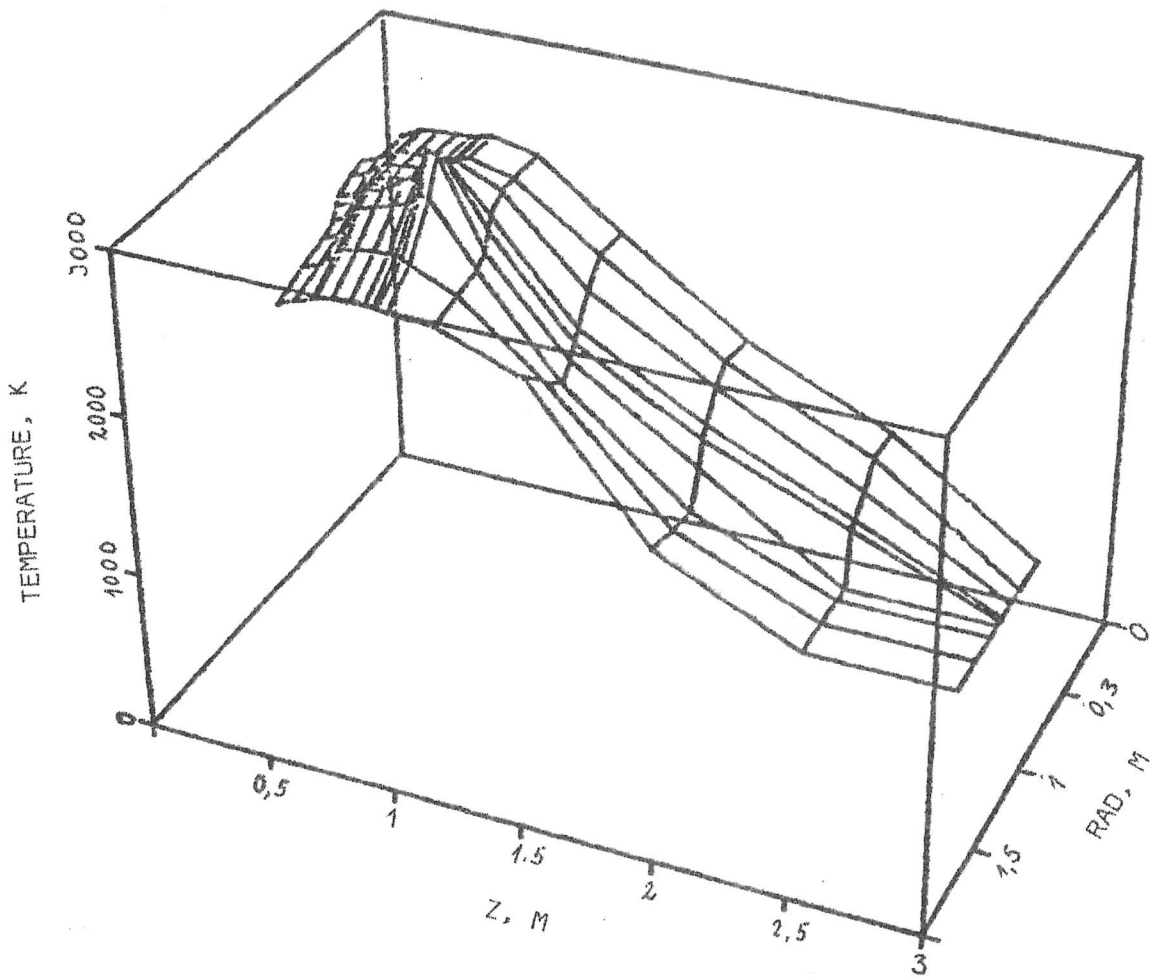


Figure 4c

PITCH = 1 , ANGLE 2

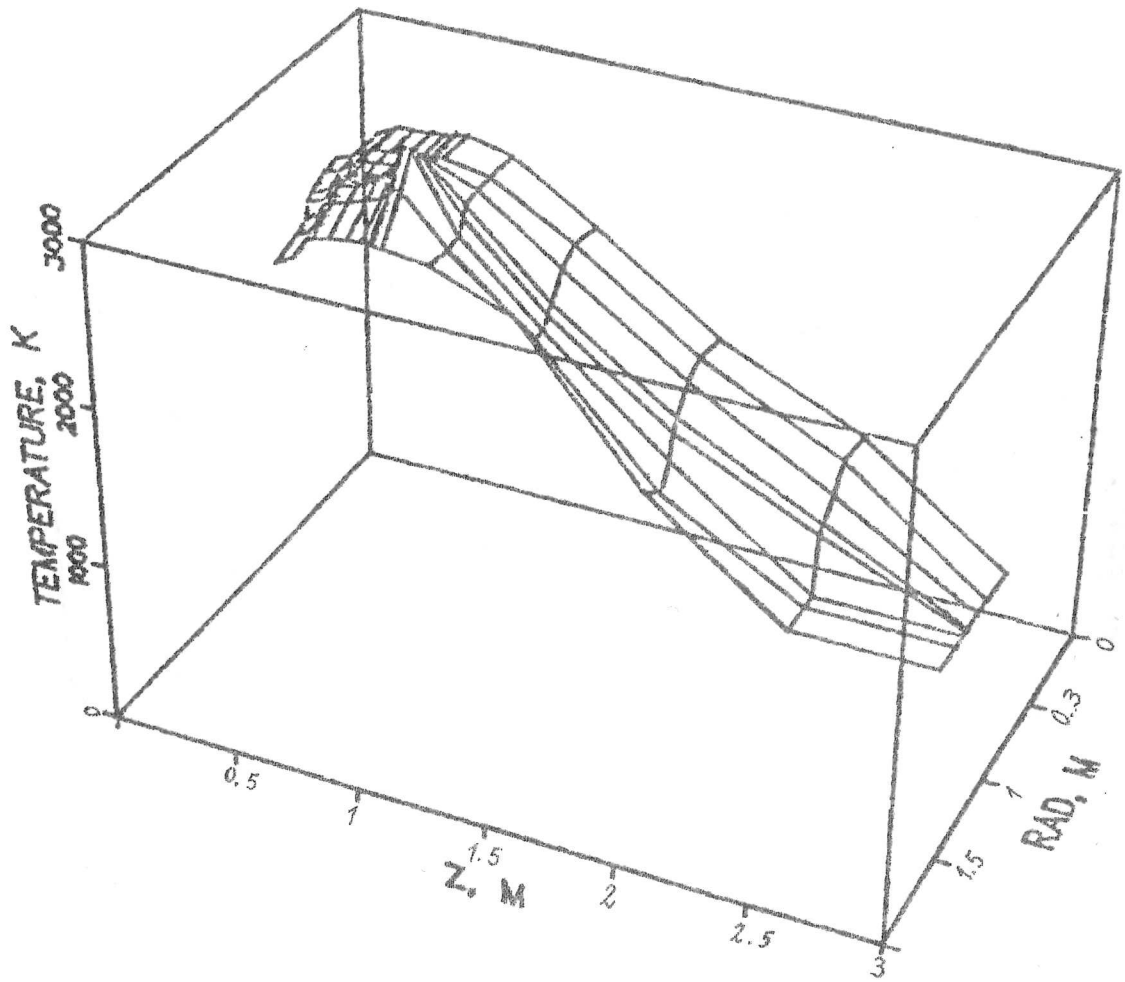


Figure 4d

BASE CASE, ANGLE 6

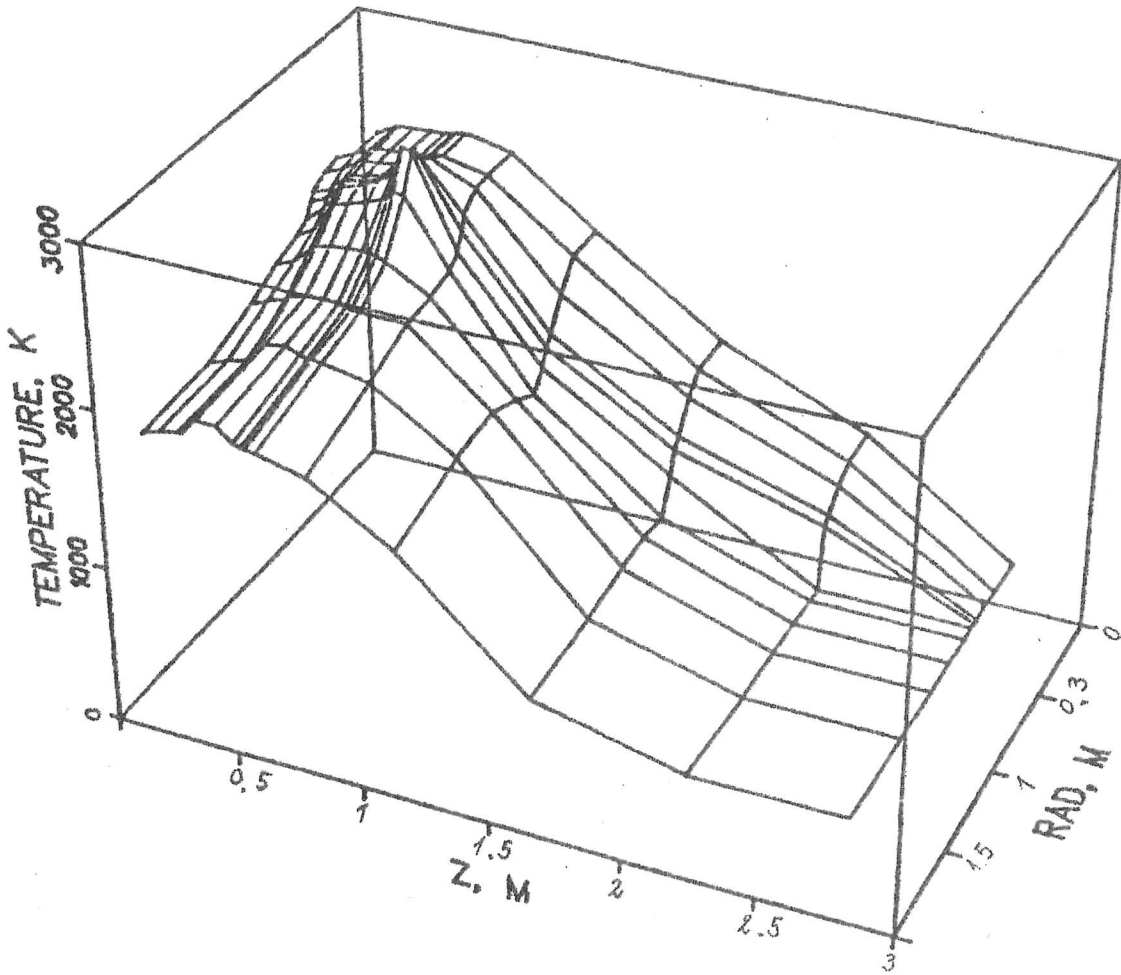


Figure 4e

FURNACE RADIUS = 2 , ANGLE 6

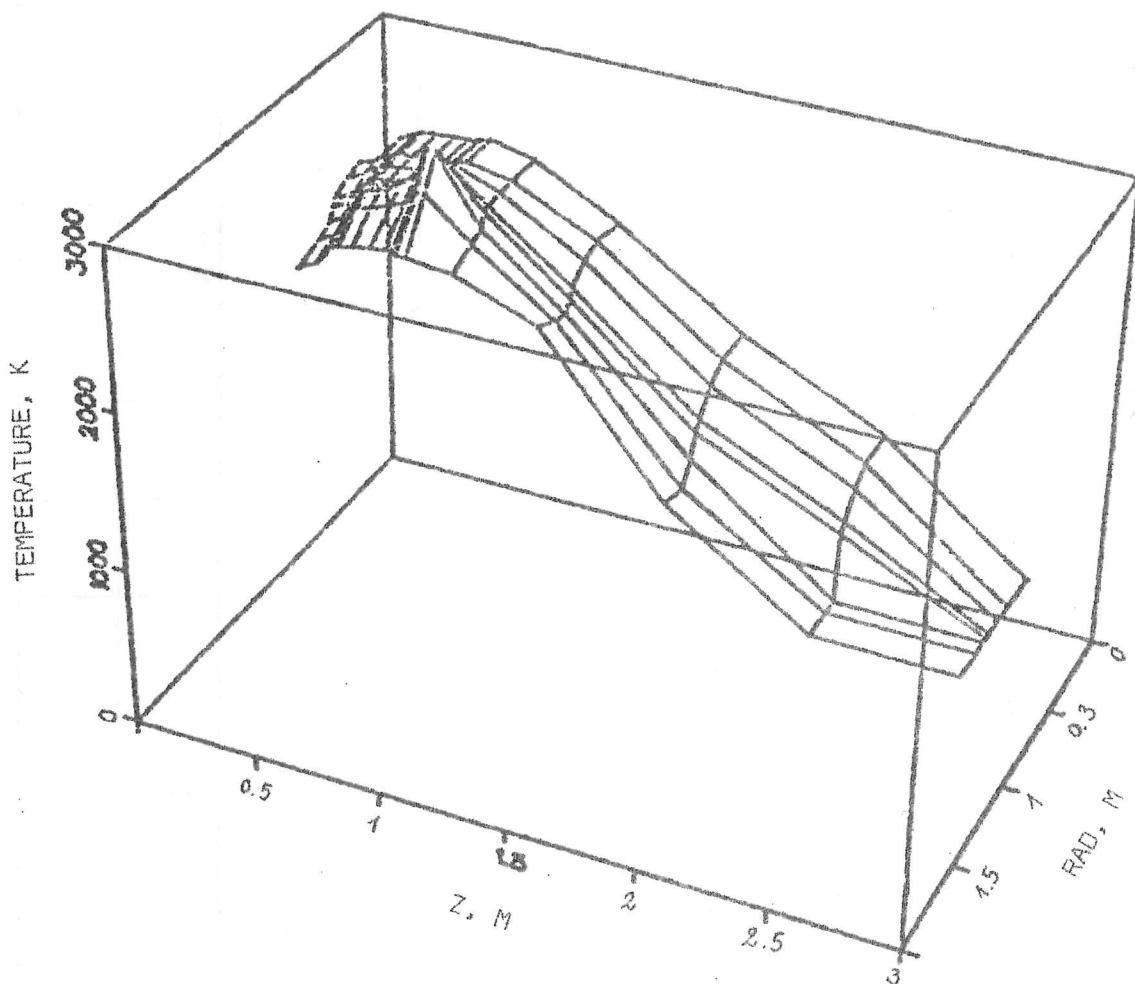
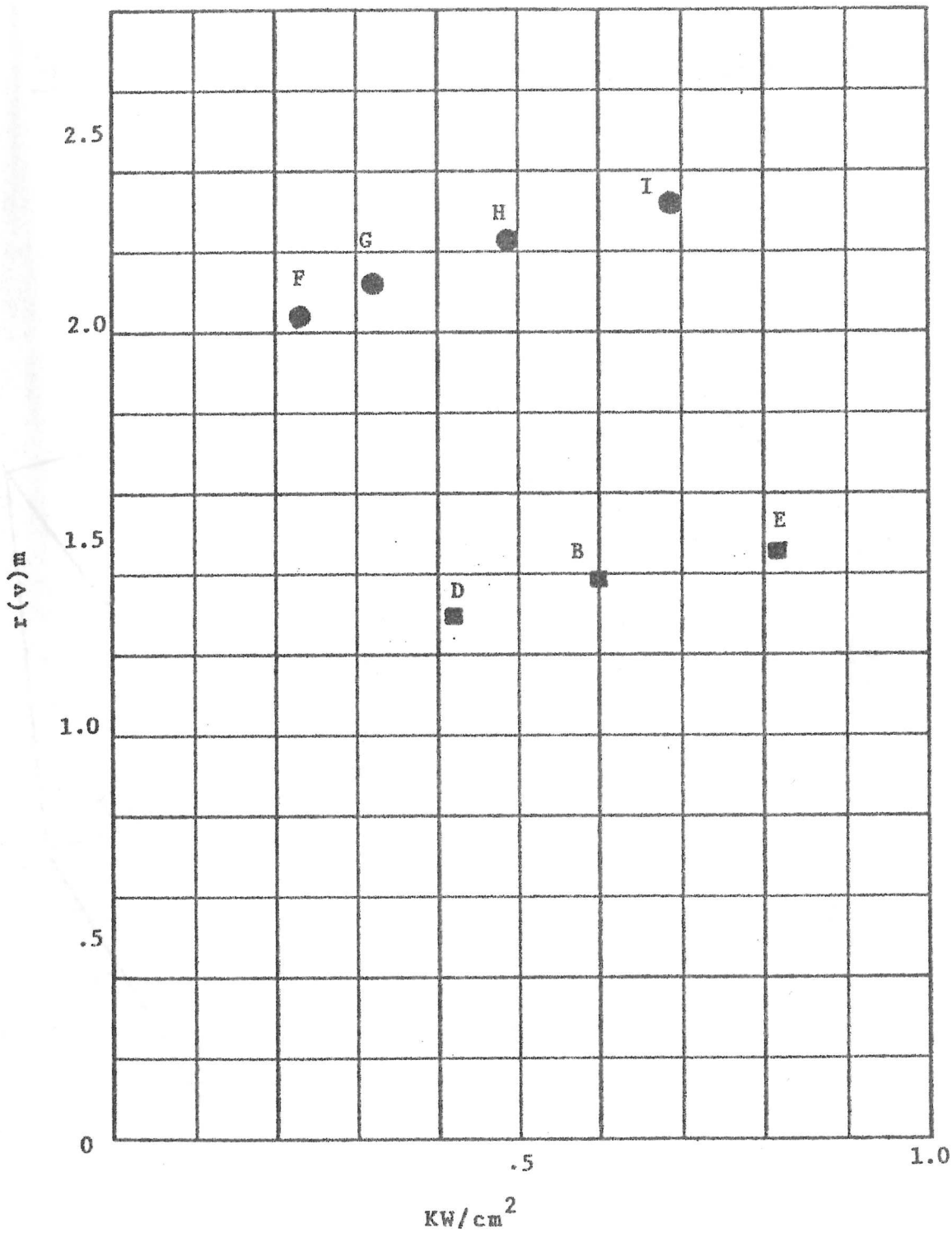


Figure 5

r(v) versus Power Density



DISCUSSION

Dr. L. Alberts*

The fact that you use the in phase voltage for your K expressing means, I assume, that you are ignoring the reactance component. Also if you extend the eddy current region below the electrode tip, that implies a reactance component. Can this be completely ignored in the model while it retains its validity?

Dr. J.H. Downing:

The reason for the exclusion of the magnetic field from the model was mathematical convenience necessitated by the extremely complicated physical problem. It was hoped that its effect would be small compared to the effect of the electrical and temperature fields. The effect of the magnetic field would be anticipated to be greatest in the electrode where it should tend to cause current to concentrate near the surface of the electrode. The neglect of the magnetic field and the assumption of only vertical flow of materials caused a crisis under the electrode because there was nothing to restrict current flow in this region and no chemical reaction to absorb the energy liberated in the subelectrode region by current flow. The introduction of a highly resistive medium under the electrode prevented current from flowing in the region and therefore also energy liberation there. This eliminated the extremely high temperatures under the electrode and permitted simulations in good agreement with observation. This device is recognised to be only a stopgap and eventually the magnetic field and non-vertical mix flow will have to be incorporated into the model.

* National Institute for Metallurgy, South Africa